

Using waste glass as a partial flux substitution and pyroplastic deformation of a porcelain stoneware tile body

E. Rambaldi ^{a,*}, W.M. Carty ^b, A. Tucci ^a, L. Esposito ^a

^a Centro Ceramico, Via Martelli 26, 40138 Bologna, Italy

^b Whiteware Research Center, New York State College of Ceramics at Alfred University, Alfred, NY 14802, USA

Received 7 September 2005; received in revised form 19 October 2005; accepted 9 December 2005

Available online 9 March 2006

Abstract

The glass phase composition of fired porcelain stoneware samples was used as a benchmark for the incorporation of waste glass into whiteware bodies. Starting from a commercial standard porcelain stoneware body mix, a new mix was prepared by partially replacing feldspathic sands with scrap soda-lime glass and additional clay, to keep the overall chemical composition, and therefore the glassy phase composition constant. The resulting bodies have similar characteristics and properties. The glassy phase compositions of the two bodies are similar and moreover do not vary significantly from the glassy phase compositions of commercial whiteware bodies studied in previous work. Pyroplastic deformation was also measured and the body containing recycled glass had significantly lower deformation compared to the standard body. This difference was attributed to poor mixing in the standard body, as is supported by the quartz particle separation distance distribution in the fired microstructure.

© 2006 Elsevier Ltd and Techna Group S.r.l. All rights reserved.

Keywords: Porcelain stoneware; Soda–lime–silica glass; Glassy phase composition; Pyroplastic deformation

1. Introduction

It was proposed that the glassy phase composition of triaxial porcelains lies on the glass formation boundary within the flux–alumina–silica $[(R_2O + RO) - Al_2O_3 - SiO_2]$ system [1]. In the case of most commercial porcelain compositions, the glass formation boundary lies in the mullite phase field so any excess of alumina crystallizes from the glass as mullite. If the glass formation boundary intersects the cristobalite phase field, it is proposed that cristobalite will form (but this has not yet been proven). The amount of glass formed during firing is determined by amount of flux $(R_2O + RO)$ and soak temperature during heat treatment and becomes constant once steady-state conditions have been reached. The flux level also precisely determines the alumina solubility in the glassy phase and the $Al_2O_3:(R_2O + RO)$ ratio has been determined to be constant over the range of firing temperatures applicable to all commercial porcelain stoneware compositions [1], and has been measured to be 1.19 ± 0.1 [2]. The silica level in the

glassy phase (on a unity molecular formula, UMF, basis) is dictated solely by the temperature, increasing with increasing temperature. Quartz dissolution is apparently independent of particle size, provided the system has sufficient time to reach steady-state during the high temperature dwell (generally observed to occur within two hours at peak temperature) [3].

To allow direct comparison of the glassy phase compositions of various whiteware compositions, the UMF, or Seger formula approach was used [4]. In the UMF approach the concentration of the glass constituents are represented using the standard R_2O , RO , R_2O_3 , RO_2 designation. The R_2O (Na_2O , K_2O , Li_2O) and RO (CaO , MgO , SrO , BaO , ZnO , PbO) components represent the fluxes; R_2O_3 represents the network modifier Al_2O_3 ; and RO_2 the glass former (SiO_2). (TiO_2 and Fe_2O_3 are ignored in these calculations due to their low concentration in typical whiteware bodies.) To calculate a UMF, all of the batch constituents are converted to a molar basis, the fluxes (R_2O and RO) levels are summed and the batch is normalized to the moles of flux. Therefore, Al_2O_3 and SiO_2 levels are represented as molar ratios to flux. In this way it is possible to rapidly decipher similarities in the glassy phase composition across broad composition ranges. Based on the quantitative phase analysis of the fired body, the composition

* Corresponding author. Tel.: +39 051534015; fax: +39 051530085.

E-mail address: rambaldi@cencerbo.it (E. Rambaldi).

of the glassy phase can be calculated precisely by subtracting the molar equivalents of the crystalline species from the overall chemical body chemistry [1].

Pyroplastic deformation, or slumping, occurs during the firing process due to several variables. Consistent with well-established creep theory, pyroplastic deformation is a function of the amount of stress exerted on the sample—similar stress levels lead to similar deformation (other factors being equal) and increasing the stress level increases the deformation. During the firing of a typical porcelain, feldspar particles react with SiO_2 from meta-kaolin to form a eutectic liquid at 990 °C, high in alkali and low in silica, creating low viscosity pockets. It is proposed that pyroplastic deformation starts at 990 °C (the feldspar-mullite-tridymite/ SiO_2 eutectic in the K_2O – Al_2O_3 – SiO_2 system) through movement in these low viscosity regions. Deformation slows significantly above ~1200 °C when quartz dissolution becomes rapid, increasing the SiO_2 level in the glassy phase, causing a corresponding increase in the glassy phase viscosity. It is also proposed that pyroplastic deformation has little to do with overall composition provided there is sufficient quartz present to saturate the glass with SiO_2 [5]. Therefore, it is proposed that improving the macroscopic homogeneity of the glassy phase during the firing process should decrease pyroplastic deformation [5,6].

In this work, a commercial porcelain stoneware body composition has been chosen as a standard material, and another body mix has been formulated introducing soda–lime–silica (SLS) glass (scrap packaging glass, obtained from urban wastes) as a partial substitution for typical feldspathic fluxing agents. Previous studies have shown that this substitution, at a level of between 5 and 10 wt.%, improve the characteristics of the porcelain stoneware tile [7,8].

Unique to this study is that the flux substitution was undertaken to match the glassy phase composition of the standard composition. The results demonstrate that this approach is valid for porcelain stoneware materials consistent with the results already reported for porcelain compositions [9]. It was also observed that samples containing substituted waste glass for feldspathic fluxes had actually less pyroplastic deformation than the standard body, a result that was attributed to poor mixing in the standard body, also consistent with previous studies [6].

2. Materials and methods

An industrial porcelain stoneware body mix, denoted GPA, was prepared as shown in Table 1. From this standard composition, an ideal body mix, denoted GPA6%, was formulated using waste glass (soda–lime–silica, SLS, glass) as a partial replacement (6 wt.%) for the feldspathic fluxing agent. In the new formulation, the molar ratios of SiO_2 and Al_2O_3 to flux (R_2O and RO) were kept constant, as indicated in Table 1. Increasing the clay level is necessary to maintain the appropriate Al_2O_3 level, because the waste glass is substantially deficient in Al_2O_3 . When the fluxes are grouped (R_2O + RO) and assumed to act similarly, the chemistry of the overall body composition, as defined by the UMF (with grouped fluxes),

Table 1

Batch compositions, calculated UMF for the bodies and slip characteristics

	GPA	GPA6%
Clay A (wt.%)	10	10
Clay B (wt.%)	38.5	53
K feldspathic sand (wt.%)	16	9
Na feldspathic sand (wt.%)	35.5	22
SLS glass (wt.%)	0	6
Na_2O (mol%)	3.66	3.14
K_2O (mol%)	1.31	1.13
MgO (mol%)	0.54	0.94
CaO (mol%)	1.19	1.48
$\text{RO} + \text{R}_2\text{O}$ (mol%)	6.70	6.69
Al_2O_3 (mol%)	12.34	12.33
SiO_2 (mol%)	80.67	80.67
UMF	1.0:1.9:12.3	1.0:1.9:12.5
Density (g/cm^3)	1.72	1.72
pH	10.17	10.13
Average particle size (μm)	10.0	9.6

does not differ significantly between the two batches. The chemical composition of the SLS glass and the other raw materials were measured using inductively coupled plasma-atomic emission spectroscopy (ICP-AES Optima 3200 XL, Perkin-Elmer, USA) and are listed in Table 2.

To prepare the batches, raw materials were dispersed in an aqueous slip containing 70 wt.% solids and 1 wt.% dispersant (sodium hexametaphosphate: $\text{Na}_6(\text{PO}_3)_6$) then ball milled for 9 h in a porcelain jar with alumina media. The GPA6% raw materials were pre-ground by hand using a mortar and pestle to eliminate particles larger than 100 μm . The SLS glass was wet ball milled one hour and was added to the other batch powders. The GPA raw materials were not pre-ground and particles were larger than 100 μm before the milling process.

Slurries were prepared and were characterized for density, pH, and particle size distribution (LA920, Horiba, USA) as listed in Table 1. The particle size distribution curves are presented in Fig. 1. The slurries were filter pressed then vacuum de-aired extruded into rods of 12.2 mm diameter and ~25 cm in length. The measured water content of the plastic bodies ranged from 18 to 23% dry weight basis (d.w.b.). The dried rods were fired in an electric furnace (Thermolyne 46200, USA) at peak temperatures ranging from 1040 to 1180 °C in 20 °C increments at a heating rate of 3 K/min and a 2 h dwell to reach steady-state conditions. The fired rods were characterized for linear shrinkage, water absorption, and apparent bulk density using a standard test method approved for ceramic tile [10]. Samples fired at 1080 and 1120 °C were polished and etched (20% HF for 10 s), then evaluated using scanning electron microscopy (SEM, 515 Philips). Fracture samples were also evaluated.

An internal standard method was used to quantify the amount of quartz and mullite in each samples by X-ray diffraction analysis (XRD Siemens, 40 kV and 30 mA) corrected for volume [2]. Fluorite (CaF_2) was chosen as the internal standard, because its diffraction peaks do not obstruct or confound quartz, cristobalite, or mullite peaks. Fired samples were ground to <45 μm using mortar and pestle. The fluorite was not

Table 2

Chemical composition (wt.%) of the raw materials used to prepare the two body mixes

	Clay A (wt.%)	Clay B (wt.%)	K feldspar (wt.%)	Na feldspathic sand (wt.%)	SLS glass (wt.%)
SiO ₂	80.46	66.75	72.35	69.81	72.80
Al ₂ O ₃	13.70	21.93	13.50	17.74	1.50
TiO ₂	0.05	1.24	0.00	0.06	0.07
Fe ₂ O ₃	0.13	0.99	1.02	0.30	0.25
CaO	0.07	0.33	2.53	1.31	9.21
MgO	0.01	0.52	0.17	0.19	3.38
K ₂ O	0.19	1.33	6.58	0.59	0.71
Na ₂ O	0.06	0.22	0.21	8.93	11.76
BaO	0.00	0.00	0.00	0.00	0.07
ZrO ₂	0.00	0.07	0.00	0.00	0.17
L.O.I. ^a	4.97	6.62	3.60	0.64	0.00

^a Loss on ignition.

ground. A mixture of glass powder, containing 10 wt.% fluorite, was created by dry mixing (C32003A, Dentsply Rinn, Elgin, IL), for 5 min, to ensure homogeneity. The powder was then analyzed using a X-ray diffractometer (Siemens D500 Goniometer with a Kristalloflex 810 X-ray generator, Philips) over the 2θ range of 15° to 60° with 0.04° step size and 4 s dwell (count time). Each diffraction pattern was analyzed using the profile-fitting function in Jade (Version 3.1, Material Data, Inc.). The three peaks of quartz, respectively (1 0 1), (1 0 0) and (1 1 2), of mullite, respectively (0 0 1), (2 2 0) and (1 2 1), and of fluorite, respectively (1 1 1), (2 2 0) and (1 1 3), were used in the analysis. To quantify the amounts of mullite and quartz present in each sample, the ratio of peak areas were compared to a previously generated calibration curve [2]. The reliability of the measurement was $\pm 2\%$ for mullite, and $\pm 3\%$ for quartz.

To calculate the composition of the glassy phase, the amounts of alumina and silica in the mullite and quartz were subtracted from the overall chemical analysis of the body. The composition of mullite is assumed to be $3\text{Al}_2\text{O}_3 \cdot 2\text{SiO}_2$. The amount of glass in the samples was then determined by adding the amount of the crystalline material and subtracting from 100%.

Pyroplastic deformation, was measured using a previous developed method in which the span is adjusted to keep the

bending, or outer fiber tensile stress (OFTS, σ_B) on the sample, is nearly constant [5]. The OFTS is obtained from Eq. (1).

$$\text{OFTS} = \sigma_B = \frac{(\rho g L^2)}{d} \quad (1)$$

where L is the span length between supports, ρ is the apparent bulk density of the fired sample, g is the acceleration due to the gravity, and d is the diameter of the rod.

Five specimens were tested at three different firing temperatures (1080, 1100, and 1120 °C), at an OFTS of 40 kPa, for both compositions (GPA and GPA6%). Unfired specimens were placed on gauge block separated at the appropriate span obtain the initial height (H_G). After firing the sample rod was placed on the same gauge blocks, the height measured again (H_F), and the diametric shrinkage (S) of the rods is measured. The pyroplastic deformation (PPD), typically reported in mm, is then [5]:

$$\text{PPD} = H_G - H_F - S \quad (2)$$

3. Results and discussion

The particle size distribution data, presented in Fig. 1, indicates that GPA6% possesses a finer and more homogeneous particle size distribution than GPA. Both bodies exhibit a bimodal distribution. The apparent uniformity of GPA6% was attributed to the raw material pre-grinding step.

Bulk density, water absorption and linear shrinkage of fired test pieces are reported in Fig. 2 for GPA and GPA6%. Replacement of the feldspathic fluxes with SLS glass, while keeping the overall flux level constant (on a molar basis), does not change the firing behavior of the porcelain stoneware material studied. Both the compositions reach a water absorption below 0.5 wt.% (0.3 and 0.2 wt.% for GPA and GPA6%, respectively) at 1080 °C. This water absorption level is necessary to satisfy the definition of a porcelain stoneware material [11,12]. Water absorption reaches 0% at higher temperatures. From Fig. 2 a and b respectively, it is possible to see that the density values are almost the same in GPA and GPA6% and the linear shrinkage shows the same trend for the

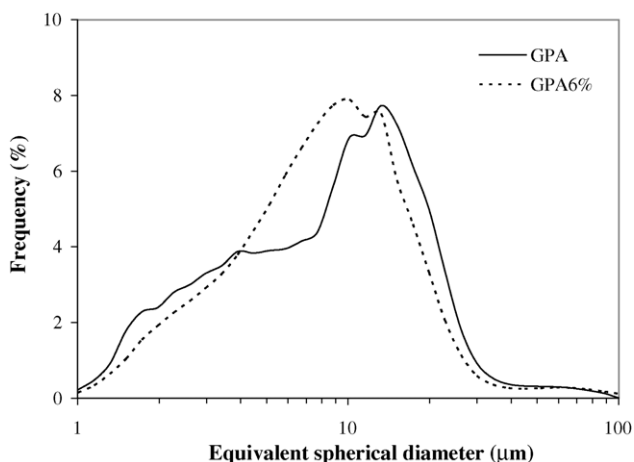


Fig. 1. Particle size distributions of the slips of GPA and GPA6%.

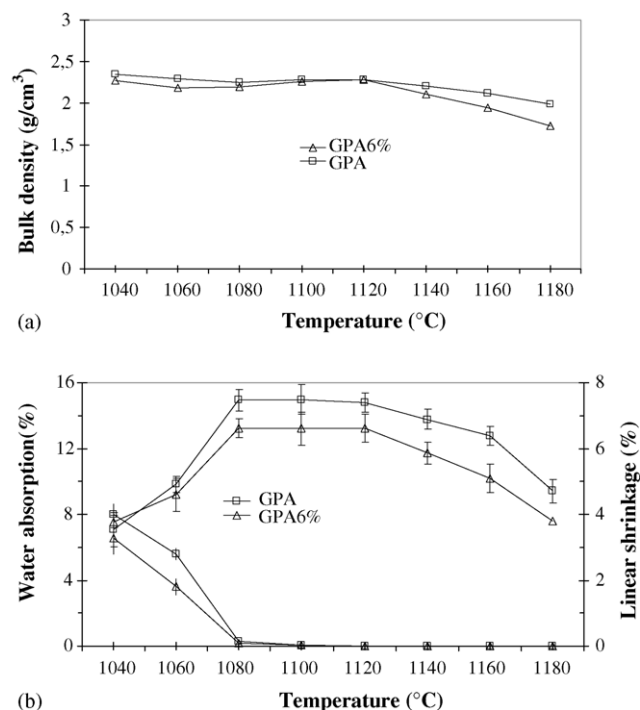


Fig. 2. (a) bulk density and (b) water absorption and linear shrinkage as a function of the firing temperature for GPA and GPA6% body mixes.

two body mixes, with a stable plateau over the range 1080 and 1120 °C. At temperatures greater than 1120 °C a slight expansion (negative shrinkage) is observed indicating the initiation of over-firing.

The bodies have similar firing behavior because their compositions were tailored to match the overall chemistry of GPA, see Table 1. Since the chemistry of the two bodies matches, it is proposed that the chemistry of the glassy phases similarly matches, consistent with previous work. These considerations are made taking into account the sum R_2O and RO , while the Na/K or Ca/Mg ratios did not seem to have a significant role, as it is indicated in Table 1, where the mole percentages of the flux oxides are reported. Specifically, the substitution of SLS glass for feldspar, with additional clay to keep the overall alumina level consistent, can be easily accomplished producing a body with similar firing behavior. Based on the data, the optimum firing temperature for these bodies is 1080 °C where the shrinkage is maximum and the water absorption is less than 0.5 wt.%. It is important to underlain as the firing schedule used in these tests, 3 K/min gradient and 2 h dwell time allowing to reach steady-state conditions, is quite different from the real conditions of firing in porcelain stoneware tile, for which rapid firing cycles are used, about 40 K/min and 5–10 min dwell time. That results interesting because porcelain stoneware tile, in these tests, probably reached steady-state conditions.

Some interconnected pores are visible in the photomicrographs in Fig. 3 at 1080 °C, although it is possible that the samples may be over-etched. Overall, the microstructure of GPA6% appears to be more homogeneous than GPA.

To evaluate the uniformity of the microstructure, the quartz particle separation distances were measured. The measurement

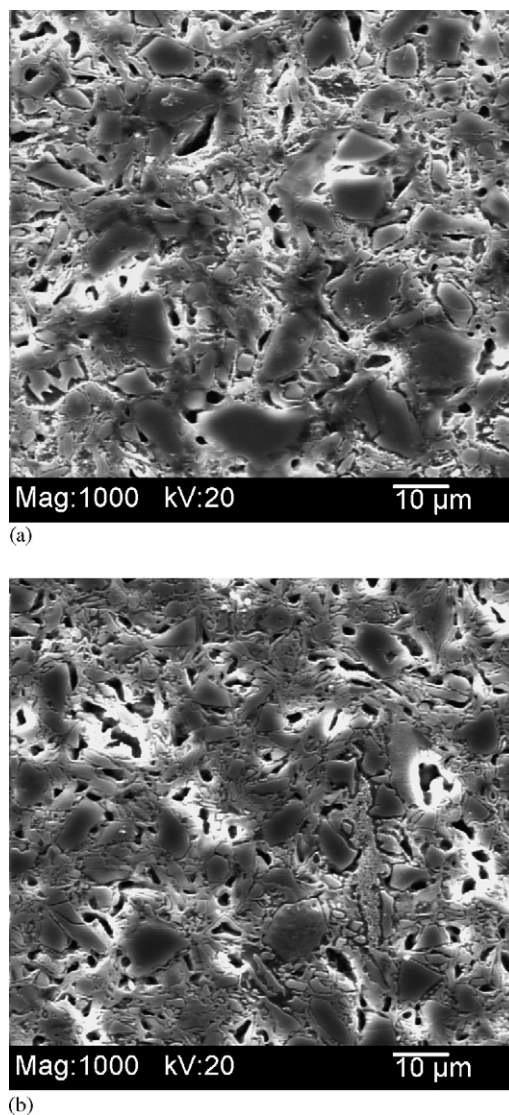


Fig. 3. SEM micrographs of the polished and etched fracture surfaces of: (a) GPA and (b) GPA6% samples, both fired at 1080 °C.

of the spacing of the quartz particles provides a unique opportunity to determine the degree of mixing in a whiteware body since undissolved quartz particles are unable to migrate during the firing process. Quartz particle clusters would produce a bimodal particle separation distribution. Fig. 4 shows quartz particle separation distance frequency curves of GPA and GPA6%. The data was obtained measuring center-to-center distances of undissolved quartz particles from SEM photomicrographs at 1080 °C (Fig. 3) and then subdividing those distances in separation classes. Eight classes were defined, from Class I with spacing of 0–5 µm to Class VIII with spacings from 36 to 40 µm. GPA possesses a bimodal distribution while GPA6% has a mono-modal distribution. GPA6% is more homogeneously mixed than GPA.

Fig. 5 shows the X-ray diffraction patterns of GPA and GPA6%, at 1080, 1100, and 1120 °C. The samples show similar trends and at the lowest temperature (1080 °C) plagioclase is still present in the bodies (but not at 1100 and 1120 °C).

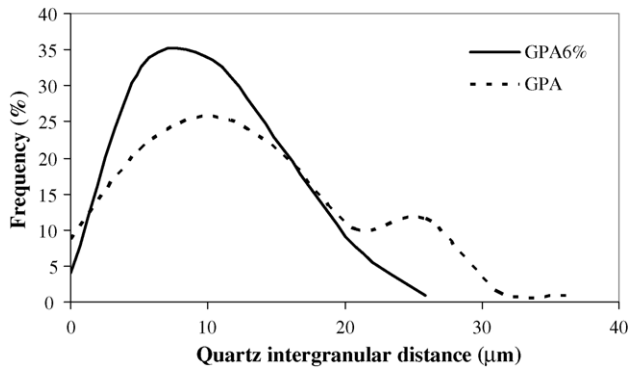


Fig. 4. Frequency of the quartz intergranular distance for GPA and GPA6% both fired at 1080 °C.

The weight percentages of the mullite and quartz are listed in Table 3. Only 1100 and 1120 °C were evaluated because plagioclase is still present at 1080 °C. Plagioclase complicates the calculation of the glass composition, as albite and anorthite form a complete solid solution series, so the level of Al_2O_3 in the glass could be variable as it is dictated by the level of Na_2O and CaO in the crystallized plagioclase. Their composition cannot be exactly calculated using the chemical data reported in Table 2, moreover some plagioclase crystals may form in GPA6% containing SLS glass, as found in previous works [7,8,13]. As illustrated in Table 3, the concentration of quartz and mullite in the two bodies is essentially identical. The quartz level is slightly greater in GPA, but is within the range of measurement error. In Fig. 6 are reported two micrographs of GPA and GPA6% at 1120 °C showing the primary and secondary mullite crystals [14].

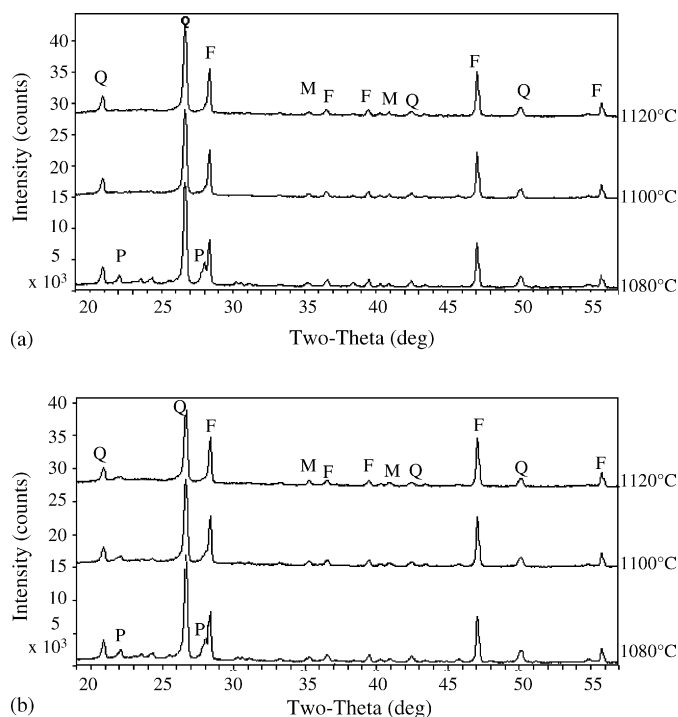


Fig. 5. X-ray diffraction patterns of: (a) GPA and (b) GPA6% body mixes at 1080 °C, 1100 °C and 1120 °C. (Q: quartz; P: plagioclase; F: fluorite; M: mullite).

Table 3

Quantitative mineralogical analyses of the two compositions, at two different temperatures in wt. %

	Mullite phase		Quartz phase		Glass phase	
	GPA ^a	GPA6% ^a	GPA ^a	GPA6% ^a	GPA ^a	GPA6% ^a
1100 °C	9.5	9.5	16.3	13.2	74.2	77.3
1120 °C	9.9	10.0	14.6	12.7	75.4	77.4

The reliability of the measurement is $\pm 2\%$ for mullite and $\pm 3\%$ for quartz.

^a Sample.

The glassy phase compositions of the samples at 1100 and 1120 °C is calculated by subtracting the crystalline contributions from the overall chemistry of the body. The chemistry of the bodies and of the glassy phases are plotted in Fig. 7. This representation is a modification of the leucite–mullite–cristobalite region phase diagram [15,16], considering the feldspars ($[\text{RO} + \text{R}_2\text{O}] \text{Al}_2\text{O}_3 \cdot 6\text{SiO}_2$), instead of leucite ($\text{K}_2\text{O} \text{Al}_2\text{O}_3 \cdot 4\text{SiO}_2$), as fluxing agents in porcelain stoneware

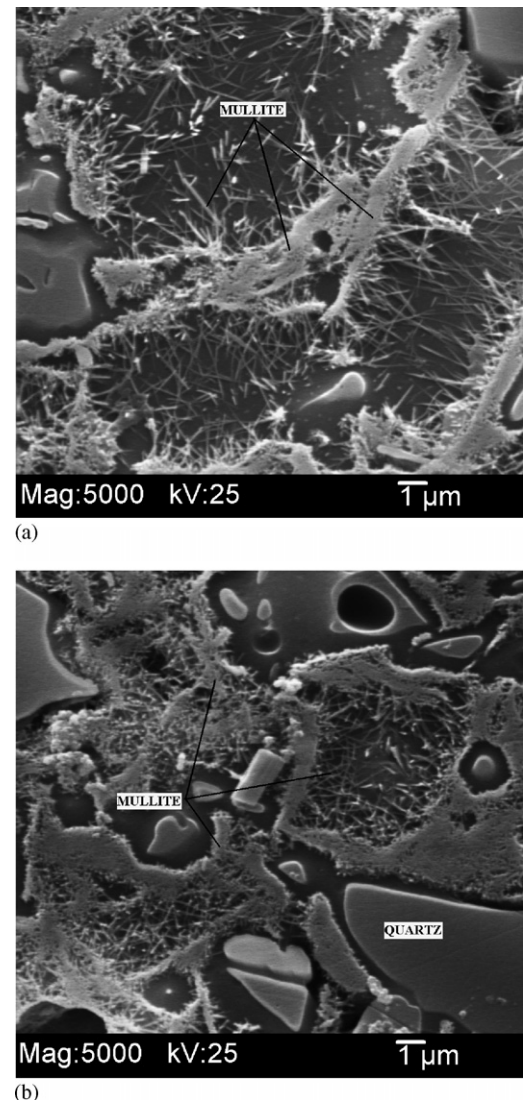


Fig. 6. SEM micrograph of mullite crystals of GPA (a) and GPA6% (b) samples at 1120 °C.

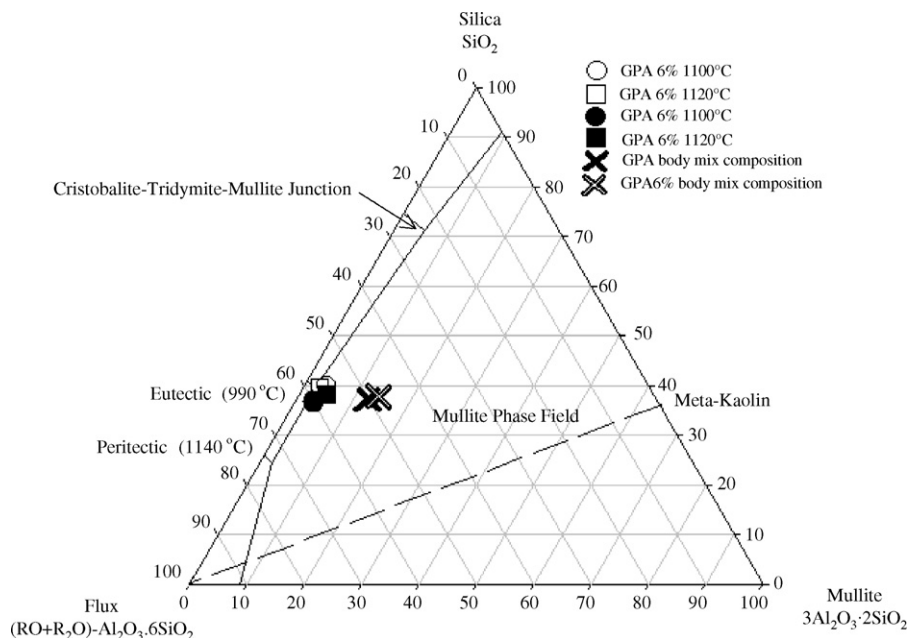


Fig. 7. Glassy phase composition of the two body mixes at two different temperatures in the flux-mullite-silica region of the $(\text{RO} + \text{R}_2\text{O})\text{-Al}_2\text{O}_3\text{-SiO}_2$ phase diagram.

Table 4

Glass phase compositions (UMF) of the samples at two different temperatures

Glass phase UMF	SiO ₂	TiO ₂	Al ₂ O ₃	Na ₂ O	K ₂ O	MgO	CaO	RO + R ₂ O
GPA 1100 °C	8.88	0.25	1.18	0.55	0.19	0.08	0.18	1.0
GPA 1120 °C	9.11	0.25	1.15	0.55	0.19	0.08	0.18	1.0
GPA6% 1100 °C	9.37	0.24	1.19	0.47	0.16	0.14	0.23	1.0
GPA6% 1120 °C	9.43	0.24	1.15	0.47	0.16	0.14	0.23	1.0
Previous work [2]			1.19 ± 0.1					

compositions. The glassy phase compositions at 1100 and 1120 °C are listed in Table 4 and demonstrate that the glassy phase does not differ significantly between the two samples and the amount of alumina is very close to the value obtained in the previous work (1.19 ± 0.1) [2]. In any case, it has to be considered that UMF approach tends to minimize variations that could be significant. The substitution of Na feldspathic sand with SLS glass, involves an increase of CaO and MgO and a decrease in K₂O and Na₂O in the glassy phase of

GPA6%. These variations are associated to a slight increase of SiO₂ in GPA6%.

Finally, pyroplastic deformation data is presented in Fig. 8 for 1080, 1100, and 1120 °C. As shown, GPA presents a higher pyroplastic deformation at all three temperatures and this is attributed to mixing heterogeneities, consistent with other work that demonstrates the pyroplastic deformation decreases as mixing effectiveness increases (Figs. 3 and 4) and with the measurement of the quartz interparticle spacing distribution (Fig. 4) [6].

4. Conclusions

It was shown that a commercial porcelain stoneware body (GPA) and a body containing SLS glass (GPS6%) exhibited similar properties, mineralogy, and firing behavior. This demonstrates that invoking the concepts of UMF, thus providing for similar overall chemistries, allowed waste glass to be incorporated as a flux source with predictable results. Mixing quality was determined by measuring the distribution apparently correlated with increased pyroplastic deformation, consistent with previous measurements of spacing between quartz particles in the fired microstructure and poor mixing.

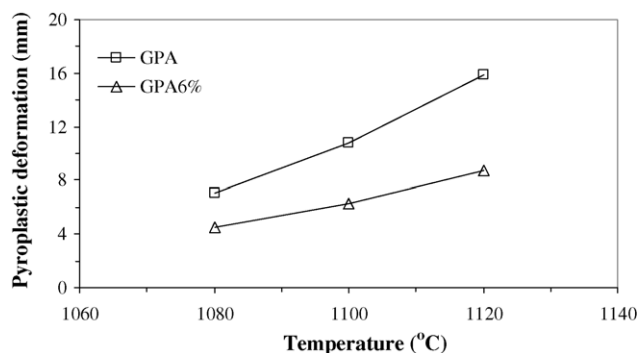


Fig. 8. Pyroplastic deformation values of the two body mixes, measured at 40 kPa, at 1080, 1100, and 1120 °C.

References

- [1] W.M. Carty, Observations in the glass phase composition in porcelains, *Ceram. Eng. Sci. Proc.* 23 (2) (2002) 79–94.
- [2] H. Lee, W.M. Carty, Glass phase composition in porcelains and correlation with firing temperature, in: *Proceedings of the 106th Annual Meeting and Exposition of the American Ceramic Society*, April 18–21 2004, Indianapolis, Indiana, USA, 2004.
- [3] B. Pinto, W. Carty, S. Misure, Measurement of residual strain in quartz particles in porcelain, *Science of Whiteware*, vol. III, Alfred University, 2000.
- [4] W. Carty, M. Katz, J. Gill, Unity molecular formula approach to glaze development, *Ceram. Eng. Sci. Proc.* 21 (2) (2000) 95–109.
- [5] A.M. Buchtel, Pyroplastic deformation of whitewares, M.S. thesis, Alfred University, 2003.
- [6] J. McCann, Effect of mixing on pyroplastic deformation, B.S. thesis, Alfred University, 2004.
- [7] A. Tucci, L. Esposito, E. Rastelli, C. Palmonari, E. Rambaldi, Use of soda-lime scrap glass as a fluxing agent in a porcelain stoneware tile mix, *J. Eur. Ceram. Soc.* 24 (2004) 83–92.
- [8] A. Tucci, E. Rambaldi, L. Esposito, Use of scrap glass as a raw material for porcelain stoneware tiles, *Adv. Appl. Ceram.* 105 (1) (2006) 40–45.
- [9] U. Kim, H. Lee, W. Carty, Development of porcelain bodies with recycled CRT glass, *J. Eur. Ceram. Soc.*, in press.
- [10] Ceramic tiles. Part 3. Determination of water absorption, apparent porosity, apparent and relative density and bulk density. International Standard ISO 10545-3, 1995.
- [11] G. Timellini, C. Palmonari, *Ceramic tile in urban design—application manual*, Edi. Cer SpA, Sassuolo, Modena, Italy, 2002.
- [12] Ceramic tiles—definitions, classification, characteristic and marking. International Standard ISO 13006, 1998.
- [13] F. Andreola, L. Barbieri, A. Corradini, I. Lancellotti, T. Manfredini, Utilisation of municipal incinerator grate slag for manufacturing porcelainized stoneware tiles manufacturing, *J. Eur. Ceram. Soc.* 22 (2002) 1457–1462.
- [14] W.E. Lee, Y. Iqbal, Influence of mixing on Mullite formation in porcelain, *J. Eur. Ceram. Soc.* 21 (2001) 2583–2586.
- [15] W.D. Kingery, H.K. Bowen, D.R. Uhlmann, *Introduction to Ceramics*, second ed., John Wiley and Sons, New York, 1976, p. 533.
- [16] E.F. Osborn, A. Muan, System $K_2O-Al_2O_3-SiO_2$; composite, in: E.M. Levin, C.R. Robbins, H.F. McMurdie (Eds.), *Phase Diagrams for Ceramists*, vol. 156, American Ceramic Society, 1964.